A Fluorescence Correlation Spectroscopy Study of the Diffusion of an Organic Dye in the Gel Phase and Fluid Phase of a Single Lipid Vesicle

Subhadip Ghosh, Aniruddha Adhikari, Supratik Sen Mojumdar, and Kankan Bhattacharyya*

Physical Chemistry Department, Indian Association for the Cultivation of Science, Jadavpur, Kolkata 700 032, India

Received: December 18, 2009; Revised Manuscript Received: March 4, 2010

The mobility of the organic dye DCM (4-dicyanomethylene-2-methyl-6-*p*-dimethyl aminostyryl-4*H*-pyran) in the gel and fluid phases of a lipid vesicle is studied by fluorescence correlation spectroscopy (FCS). Using FCS, translational diffusion of DCM is determined in the gel phase and fluid phase of a single lipid vesicle adhered to a glass surface. The size of a lipid vesicle (average diameter ~100 nm) is smaller than the diffraction limited spot size (~250 nm) of the microscope. Thus, the vesicle is confined within the laser focus. Three lipid vesicles (1,2-dilauroyl-*sn*-glycero-3-phosphocholine (DLPC), 1,2-dimyristoyl-*sn*-glycero-3-phosphocholine (DMPC), and 1,2-dipalmitoyl-*sn*-glycero-3-phosphocholine (DPPC)) having different gel transition temperatures (−1, 23, and 41 °C, respectively) were studied. The diffusion coefficient of the dye DCM in bulk water is ~300 $\mu m^2/s$. In the lipid vesicle, the average D_t decreases markedly to ~5 $\mu m^2/s$ (~60 times) in the gel phase (for DPPC at 20 °C) and 40 $\mu m^2/s$ (~8 times) in the fluid phase (for DLPC at 20 °C). This clearly demonstrates higher mobility in the fluid phase compared with the gel phase of a lipid. It is observed that the D_t values vary from lipid to lipid and there is a distribution of D_t values. The diffusion of the hydrophobic dye DCM ($D_t \sim 5$ $\mu m^2/s$) in the DPPC vesicle is found to be 8 times smaller than that of a hydrophilic anioinic dye C343 ($D_t \sim 40$ $\mu m^2/s$). This is attributed to different locations of the hydrophobic (DCM) and hydrophilic (C343) dyes.

1. Introduction

In recent years, fluorescence correlation spectroscopy (FCS) has been developed as an extremely powerful technique to study biological systems at the single molecule level with high spatial resolution.[1] FCS is frequently used to determine the local concentration, diffusion coefficient of biomolecules, and various other physical parameters that can generate fluorescence fluctuations.[1] Fluorescence correlation spectroscopy (FCS) has recently been applied to study the binding of ligands to a protein,[2a,b] protein−protein interactions,[3a,b] DNA hybridization,[4] polymer chain reactions,[5a,b] DNA−protein interactions,[6a,b] interactions with receptors,[7a,b] and supramolecular complexes.[8] Zettl et al. studied the formation of micelles by FCS.[9] They showed that FCS could be used for determination of cmc in ionic surfactant systems provided attractive ionic interactions exist between the surfactant and the noncovalent dye molecule. Very recently, Lioi et al. employed FCS to study the interaction of DNA with catanionic vesicles as a means of electrostatic molecular sequestration.[10] Mueller et al. investigated the scope of encapsulating hydrophobic solutes in block copolymer vesicles.[11] Most recently, we have studied the region dependence of D_t in the gel phase of a triblock copolymer.[12] The gel consists of interpenetrating micellar aggregates of ~20 nm size.[13] The spatial resolution of a microscope is 0.61λ/NA (NA, numerical aperture = 1.2, in our case), which is ~250 nm for excitation at 470 nm. Thus, in principle, it is not possible to spatially resolve different regions of a micellar aggregate of ~20 nm size. To overcome this, we used three probes with different polarities.[12] These three probes (DCM, C343, and C480) exhibit similar D_t values in water. In the gel phase of the triblock copolymer, D_t of the hydrophobic DCM (1 $\mu m^2/s$) is found to be 29 times smaller than that of the hydrophilic probe C343 ($D_t \sim 29$ $\mu m^2/s$). To explain this, it is proposed that the highly hydrophobic DCM "walks" through the interpenetrating polymer chains.[12] The highly polar probe C343 diffuses through the water filled "void" space inside the gel and hence exhibits a higher value of D_t.[12] In this work, we will show that D_t values in different locations of a lipid also vary.

A lipid vesicle, i.e., a "water pool" surrounded by a bilayer membrane, is a simple model of a biological cell. Thus, study of diffusion in a lipid has fundamental implications in cell biochemistry.[14] In general, a lipid vesicle exhibits a well-defined phase transition temperature (T_m). Above T_m, the lipid remains in the "fluid" phase with enhanced mobility. Below T_m, a "gel" or "solid" phase is obtained with markedly reduced mobility. Hochstrasser and co-workers studied the interaction of Nile Red molecules with lipid vesicles using high spatial resolution ("single-molecule-like").[15] The lipid vesicles used in their study were of a size (~100 nm) smaller than the focal spot of the excitation source.[15] They investigated the bimolecular association and dissociation reactions of single Nile Red molecules with lipid vesicles from an analysis of the on-and-off fluctuations in the fluorescence signal.[15] They, however, did not study diffusion of Nile Red in the lipid by FCS.[15]

Korlach et al.[16] previously applied FCS to determine D_t of an organic molecule in different phases of giant unilamellar vesicles of size >25 μm. They used different ratios of DLPC/DPPC to obtain the different phases (fluid or ordered) of the lipid bilayer at the same temprature. In the DLPC (no DPPC), only a single fluid phase (low viscosity) was observed. On increasing the DPPC content (i.e., DLPC/DPPC = 0.6/0.4), an ordered phase (high viscosity) was shown to coexist with the fluid phase. FCS studies reveal that, at a high DLPC/DPPC (>0.8/0.2) ratio, only the fluid phase is present and the

* To whom correspondence should be addressed. E-mail: pckb@iacs.res.in.

10.1021/jp911971p
Published on Web 04/13/2010

SCHEME 1: Schematic Representation of (A) DCM, (B) C480, and (C) C343

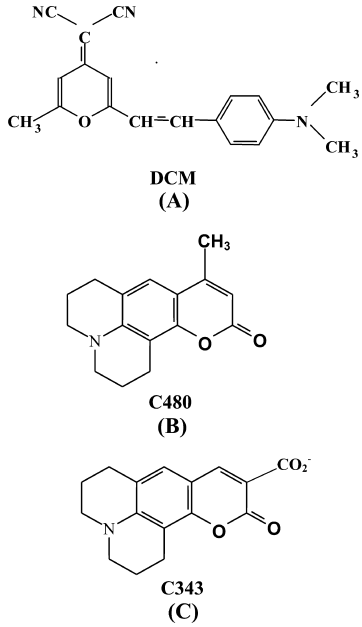

autocorrelation curve is marked by fast diffusion ($D_t \sim 4 \times 10^{-8}$ cm^2/s). Though this study indicated a variation of mobility of different phases, they did not generate a gel phase, exclusively. At a low DLPC/DPPC (<0.7/0.3) ratio, they observed that both of the phases (fluid and ordered) coexist and an additional slow component (due to the gel phase) of diffusion was detected.[16] Hof and co-workers employed FCS to study diffusion in giant unilamellar vesicles and supported phospholipid bilayers.[17,18] They reported 2-fold slower lipid diffusion in the supported bilayer compared to GUV.[17,18]

In the present work, we have studied the diffusion of an organic dye molecule (DCM) in DLPC, DMPC, and DPPC by the single molecule technique. Lipid vesicles having sizes (average diameter ~100 nm) smaller than the diffraction-limited spot size of the laser beam have been prepared. The decay of the autocorrelation function (explained later in section 2.2) originating from fluorescence fluctuations can be related to the lateral diffusion of a probe molecule within the confocal volume. Characterization of the diffusion coefficient of a dye molecule provides valuable insight into the microenvironment of the system under investigation. Our work reveals that the diffusion coefficient of the dye retards considerably as the phase of the bilayer changes from fluid to gel at room temperature. Unlike Korlach et al.,[16] we could study the pure gel phase and thus could decipher the phase dependence of mobility. To the best of our knowledge, this is the first work of FCS study in vesicles (smaller than the laser diffraction limit) at the single vesicle level and the phase dependence of D_t.

2. Experimental Section

Laser-grade dyes, 4-dicyanomethylene-2-methyl-6-*p*-dimethyl aminostyryl-4*H*-pyran (DCM, Scheme 1A), coumarin 480 (C480, Scheme 1B), and coumarin 343 (C480, Scheme 1C) were purchased from Exciton Inc. and used without further purification. We used ~2 nM dye concentration for our FCS measurements.

The lipids 1,2-dilauroyl-*sn*-glycero-3-phosphocholine (DLPC), 1,2-dimyristoyl-*sn*-glycero-3-phosphocholine (DMPC), and 1,2-dipalmitoyl-*sn*-glycero-3-phosphocholine (DPPC) were purchased from Avanti Polar Lipids and used without further purification. The phase transition temperatures of DLPC, DMPC, and DPPC are −1, 23, and 41 °C, respectively. These lipids carry zero net charge at pH 7.4. 100 μL of the sample solution was allowed to equilibrate for about 10 min before measurements were taken. The microscope cover glasses (Gold Seal, USA) were used as received without further treatment. The lipid vesicles are found to spontaneously adhere to the slides. The immobilization is confirmed by the repeated observation of the image at 15 min intervals. It is found that lipids are stationary within the time of the scan.

2.1. Vesicle Preparation. The lipid vesicles were prepared following the protocol described in ref 15. Briefly, large unilamellar vesicles were prepared by depositing a thin film of the phospholipids (typically 0.25 mL of 25 mg/mL DLPC, DMPC, and DPPC in chloroform) through the evaporation method. This was subsequently hydrated in 4 mL of phosphate buffer (20 mM, pH 7.0) with vigorous stirring at 30 °C for about an hour. Heating was used for DPPC because of its higher transition temperature. The vesicles so obtained were subjected to five freeze/thaw cycles. Then, they were extruded about 20 times through polycarbonate membranes having 100 nm pore diameter (Avanti Mini-Extruder). The concentration of the vesicles used in the single molecule experiments was ~1 pM to ensure that individual vesicles adsorbed on the glass surface stayed well isolated from one another.

The volume for a molecule of DMPC is reported[14b] to be 1100 Å^3, while the bilayer thickness is ~45 Å. For a lipid vesicle of 500 Å radius (diameter ~100 nm) the aggregation number turns out to be 117 000. For DMPC, the molecular weight is 678. We took 0.25 mL of 25 mg/mL of the lipid vesicle in chloroform, and the evaporated film was hydrated with 4 mL of phosphate buffer. This amounts to a lipid concentration of 2.3 mM. Using an aggregation number of 117 000, the vesicle concentration would be ~20 nM. This was subsequently diluted to obtain ~1 pM vesicle concentration.

2.2. Microscopy. FCS studies of the samples (~1 pM lipid vesicle, ~2 nM DCM) were carried out in a confocal setup (PicoQuant, MicroTime 200) with an inverted optical microscope (Olympus IX-71). A water immersion objective (60×, 1.2 NA) was used to focus the excitation light 470 nm (for DCM) and 405 nm (for C480 and C343) from a pulsed diode laser (PDL 828-S "SEPIA II", PicoQuant) onto the sample placed on a coverslip. After collecting the fluorescence along the same path, it was allowed to pass through a dichroic mirror and appropriate bandpass filters. We used a filter (HQ500lp for 470 nm and HQ430lp for 405 nm) to block the exciting light. To detect the fluorescence, a suitable bandpass filter (HQ580/70 m for 470 nm and HQ480/40 m for 405 nm) was used. The fluorescence was then focused through a pinhole (50 μm) onto a beam splitter prior to entering two single-photon counting avalanche photodiodes (SPADs). The fluorescence autocorrelation traces were recorded by using two detectors (SPADs). The signal was subsequently processed by the PicoHarp-300 time-correlated, single photon counting card (PicoQuant) to generate the autocorrelation function, $G(\tau)$. Data analysis of individual correlation curves was performed by using the SymPhoTime software supplied by PicoQuant. The correlation function $G(\tau)$ of the fluorescence intensities is given by[1e]

$$G(\tau) = \frac{\langle \delta F(0) \delta F(\tau) \rangle}{\langle F \rangle^2} \quad (1)$$

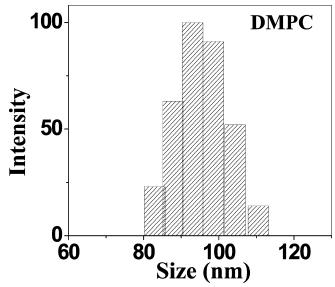

Figure 1. Size distribution of DMPC lipid vesicle as obtained through DLS studies. The vesicles were extruded through a polycarbonate membrane filter of 100 nm pore.

where $\langle F \rangle$ is the average intensity and $\delta F(\tau)$ is the fluctuation in intensity at a delay τ around the mean value, i.e., $\delta F(\tau) = \langle F \rangle - F(\tau)$.

In order to fit the correlation functions, we used the 3D diffusion model with a triplet contribution (SymPho Time). For K fractions of dye diffusing within a system with distinct diffusion constants, the correlation function $G(\tau)$ is given by[1e]

$$G(\tau) = \frac{1 - T + T\exp(-\tau/\tau_{tr})}{N(1-T)} \sum_{i=1}^{K} \phi_i (1 + \tau/\tau_i)^{-1} \times (1 + \tau/\tau_i S^2)^{-1/2} \quad (2)$$

In the above equation, τ_i denotes the average time a dye molecule resides in the confocal volume, τ_{tr} is the lifetime of a dye molecule in its triplet state, τ is the delay or the lag time, N is the average number of molecules in the excitation volume, and T indicates the fraction of molecules in the triplet state. S ($=w_z/w_{xy}$) is the structure parameter of the excitation volume; w_z and w_{xy} are the longitudinal and transverse radii, respectively. The structure parameter (S) of the excitation volume was calibrated using a sample (R6G in water) of known diffusion coefficient ($D_t = 426\ \mu m^2\ s^{-1}$).[1d] The estimated volume of the excitation volume is ~0.8 fL with a transverse radius (w_{xy}) of ~305 nm. The diffusion constant (D_t) was calculated from the following equation:

$$\tau_i = \frac{w_{xy}^2}{4D_t} \quad (3)$$

All the FCS and microscopy measurements were done at 20 °C. Images were generated using the ImageJ software.

The dynamic light scattering studies were carried out in a Brookhaven BI-200SM Goniometer (Brookhaven Instruments Corporation) with a 35 mW He−Ne laser (633 nm). The mean diameter was determined using the non-negativity constrained least-squares algorithm.

3. Results and Discussion

3.1. Dynamic Light Scattering (DLS) Study of Extruded Vesicles. Figure 1 shows the size distribution of DMPC lipid vesicles as obtained in a dynamic light scattering (DLS) study. The vesicles were extruded through a polycarbonate membrane filter of 100 nm pore. From Figure 1, it is evident that the size of the vesicles varies from ~80 to 110 nm with an average diameter of ~100 nm. A similar distribution of size is also observed for the other lipid vesicles, DLPC and DPPC.

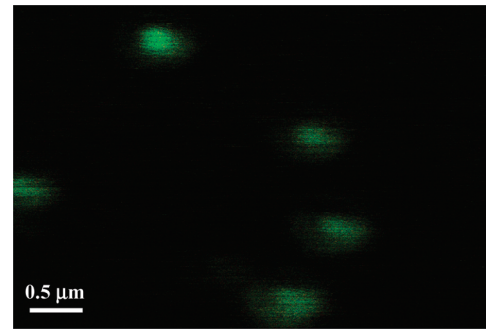

Figure 2. Confocal fluorescent images of single DPPC vesicles immobilized on a glass surface obtained by objective scanning at 20 °C. 100 μL of 20 mM phosphate buffer solution (pH 7.0) containing ~1 pM lipid vesicle and ~2 nM DCM was used. The image size is 4.5 μm by 3 μm.

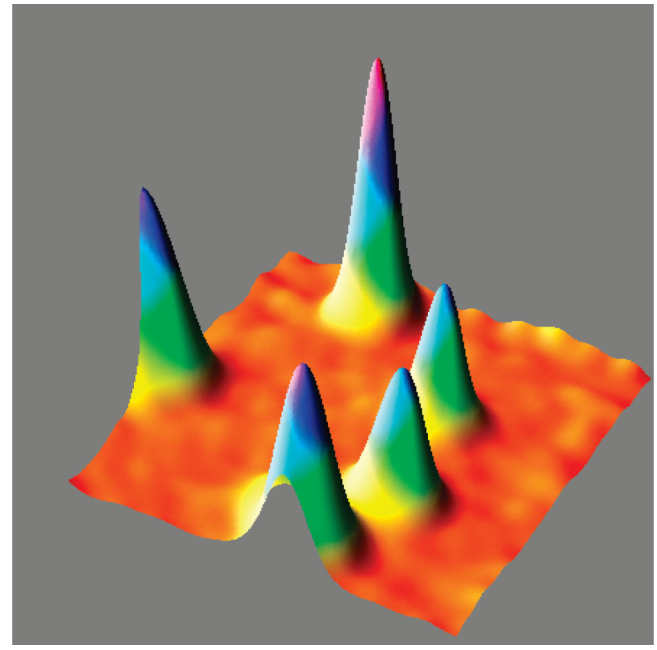

Figure 3. Confocal image (4.5 μm by 3 μm) of single DPPC vesicles dispersed on the glass surface. Each subdiffraction peak (full width at half-maximum, ~500 nm) comes from a single vesicle.

3.2. Confocal Image of the Single Lipid Vesicles. In this section, we discuss the images of individual lipid vesicles obtained using the confocal microscope. We have used a low lipid concentration (~1 pM), whereas the dye (DCM) concentration is ~2 nM. In the absence of DCM, lipid vesicles do not emit fluorescence. In the presence of a lipid vesicle, a large number of the hydrophobic DCM molecules accumulate inside the lipid vesicle and this leads to enhanced DCM emission.

Figure 2 shows a confocal image of individual DPPC vesicles adsorbed on a glass surface. The sequential scanning images at 15 min intervals exhibit the same position for the individual lipid vesicles on the glass surface. This confirms proper immobilization of the lipid vesicles on the glass surface. Thus, the vesicles remain stationary during the time of data acquisition. Single lipid vesicles confined in a volume smaller than the diffraction limited spot size of the laser beam lead to a Gaussian distribution of single vesicle fluorescence intensity (Figure 3). The average diameters of the vesicles were independently confirmed by DLS studies and found to be ~100 nm (Figure 1). The transverse radius of the excitation volume w_{xy} was determined to be ~305 nm using the D_t value for free R6G (426 $\mu m^2/s$).[1d] This implies that the width of the beam waist is

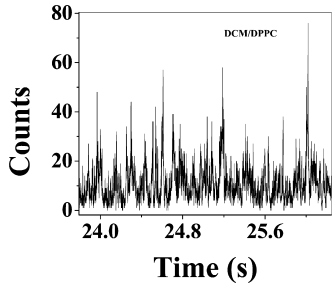

Figure 4. Typical fluorescence intensity−time record of fluorescence bursts of ∼2 nM DCM in ∼1 pM DPPC vesicle.

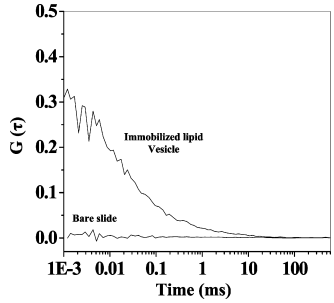

Figure 5. Comparison of the autocorrelation function obtained from DCM diffusing through a vesicle immobilized on a glass surface with that from a bare slide.

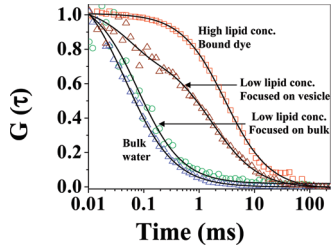

Figure 6. Autocorrelation functions of DCM at 20 °C with DMPC vesicle: (a) 0 M lipid bulk water; (b) low lipid concentration (∼10^{-12} M), focused on bulk; (c) low lipid concentration (∼10^{-12} M), focused on immobilized lipid vesicle; (d) high lipid concentration (∼10^{-7} M), focused on bulk.

at least 2 × 305 nm ≈ 600 nm and is much larger than the individual lipid vesicles (∼100 nm). Hence, the fluorescence spots in Figure 2 originate from single lipid vesicles. DCM molecules were observed to associate with and dissociate from individual lipid vesicles adsorbed on a glass surface, as endorsed by the fluctuations in fluorescence signal. Figure 4 represents how the fluorescence intensity of DCM inside the adsorbed lipid changes with time. The fluctuations obtained when the objective is focused on the vesicle are markedly different from that when focused on a bare slide. In fact, there is complete lack of correlation in the latter (Figure 5).

3.3. FCS Study of Binding of DCM with Lipid Vesicles: Effect of Concentration. The diffusion constant of DCM in bulk water is found to be quite high (300 $\mu m^2/s$).[12] We used ∼2 nM DCM and ∼1 pM vesicle concentration in our experiments. Such a low concentration of the dye and lipid vesicle leads to an insufficient binding, leaving a fraction of DCM molecules in the bulk buffer. The diffusion of free DCM in bulk water (buffer) was studied by focusing the laser beam on the bulk (Figure 6). As shown in Figure 6, for ∼2 nM DCM and ∼1 pM DMPC vesicle, the D_t value of DCM is ∼250 $\mu m^2/s$. This is close to the D_t value of DCM in pure water (300 $\mu m^2/s$) as reported earlier.[12]

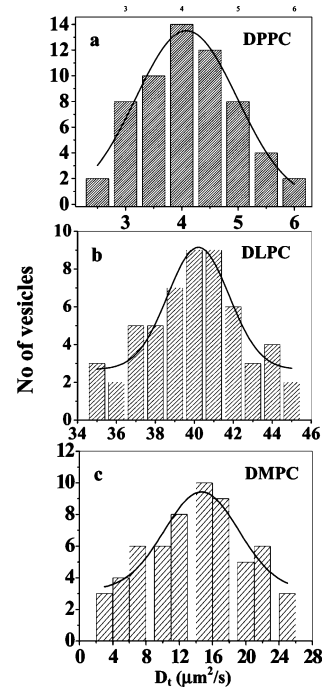

Figure 7. Distribution of D_t values obtained by analyzing around ∼60 individual (a) DPPC, (b) DLPC, and (c) DMPC vesicles. The mean value of D_t was determined by fitting the distributions to a Gaussian.

However, when the exciting laser beam was focused on individual lipid vesicles immobilized on a glass surface, we observed a markedly slower diffusion (average D_t ∼15 $\mu m^2/s$). This is 20 times slower than that obtained for free DCM in bulk water (250 $\mu m^2/s$) (Figure 6). This suggests slower diffusion of DCM inside the vesicle.

When the concentration of lipid vesicle is increased (DCM ∼ 60 nM, DMPC vesicle ∼0.6 μM), all of the probe DCM molecules bind almost entirely to the lipid vesicles. In this case, slow diffusion (D_t ∼ 7 $\mu m^2/s$) is observed even when the laser is focused on the bulk (Figure 6). The smaller D_t (7 $\mu m^2/s$) in bulk may be attributed to the diffusion of the entire lipid vesicle (∼100 nm) in bulk. It may be noted that the Stokes−Einstein equation predicts a D_t value of ∼4 $\mu m^2/s$ for a lipid vesicle of ∼100 nm size.

In summary, the D_t values obtained when we focus on individual lipid vesicles immobilized on a glass surface are markedly different from those obtained in the bulk.

3.4. FCS of DCM in Immobilized Lipid Vesicles: Distribution of Diffusion Constants. When we examined the FCS of individual vesicles, a distribution of the diffusion coefficients (D_t) was obtained (Figure 7). The D_t distribution for each type of lipid was fitted to a Gaussian shape, and the mean obtained was taken as an estimate of the average D_t (Figure 7). Such a distribution points to the presence of microheterogeneity in the lipid population, and the fluctuation in D_t values may be attributed to size and shape variation of individual lipid vesicles. The heterogeneity may originate from several sources. Boxer and co-workers have shown that the LUVs may undergo substantial distortion on adsorption to glass surfaces.[19] They detected coexistence of partially ruptured vesicles, bilayer disks along with intact lipid vesicles.

The D_t distribution is in marked contrast to ensemble average studies where a unique D_t value is expected. The spread of the D_t values for the different lipid phases also appears to be distinct. It may be noted that in the case of DMPC we observed a

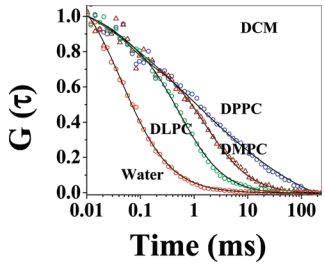

Figure 8. Autocorrelation function of DCM (~2 nM) in immobilized DPPC (~1 pM), DMPC (~1 pM), and DPPC (~1 pM) vesicles and bulk water (without lipid).

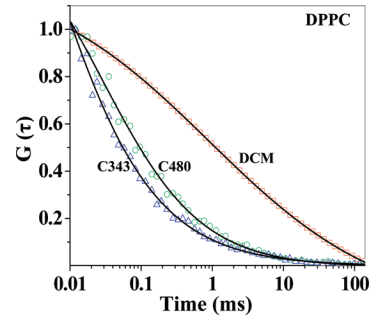

Figure 9. Autocorrelation functions of (a) C343 (~2 nM), (b) C480 (~2 nM), and (c) DCM (~2 nM) in immobilized DPPC (~1 pM) vesicles.

somewhat wider distribution of D_t values compared to either DPPC or DLPC. This may be ascribed to the fact that both the fluid and gel phases are expected to coexist for DMPC (T_m = 23 °C) near the temperature of our experiments (~20 °C).

3.5. Comparison of Gel and Fluid Phases. We have previously reported that the D_t value of DCM in bulk water is 300 $\mu m^2/s$.[12] Substantially slower diffusion (smaller D_t) was observed in the lipid vesicles. For instance, for DPPC (which remains in the gel phase at 20 °C), the average D_t value is found to be 5 $\mu m^2/s$ which is 60 times smaller than that in bulk water. In contrast, for DLPC (fluid at 20 °C), the average D_t value of DCM is 40 $\mu m^2/s$. This is 7 times smaller than that of DCM in the bulk.

The D_t distribution for each type of lipid was fitted to a Gaussian, as discussed in the above section. The distribution leads to an average D_t value (at 20 °C) of 40, 15, and 5 $\mu m^2/s$, respectively, for DLPC, DMPC, and DPPC (Figure 8). Thus, we observed a marked retardation in the diffusion coefficients (~8 times) as we moved from a lipid in the fluid phase (DLPC) to a lipid in the gel phase (DPPC).

At 20 °C, DPPC and DLPC should be almost entirely in the crystalline gel and fluid phase, respectively.[14a,20,21] The distribution of D_t values for individual DPPC vesicles has a spread from 2 to 6 $\mu m^2/s$ with a mean around 4 $\mu m^2/s$, while that for DLPC has a mean of ~40 $\mu m^2/s$ (Figure 7). The distribution of D_t for DMPC is relatively broad in contrast (Figure 7). The phase behavior of supported DMPC bilayers has widely been studied by several groups.[20,21] Atomic force microscopy (AFM) studies reveal that the DMPC vesicles reside with a complex multiphase where fluid and gel phases coexist at room temperature. The possibility of the gel transition temperature (T_m) influencing the distribution of "on-time" fluctuations in the case of DMPC (T_m = 23 °C) compared to SOPC vesicles (T_m = 6 °C) has been suggested earlier by Hochstrasser and co-workers.[15]

3.6. Probe Dependence in Lipids. Since the individual lipid vesicles (~100 nm) are smaller than the spot size (of the laser), one may argue that the observed FCS trace may be due to diffusion of the vesicle as a whole and not from diffusion of dye in the vesicle. In order to examine this, we studied diffusion of three dyes having different hydrophobicities (DCM, C480, and C343) in a single lipid vesicle (DPPC). The D_t value of C343 in bulk water (600 $\mu m^2/s$) is similar to that (550 $\mu m^2/s$) of C480 and is twice that (300 $\mu m^2/s$) of DCM in bulk water.[12] If the observed FCS trace were due to diffusion of the vesicle, one would expect similar variation (only 2-fold) of D_t for the three dyes in a lipid vesicle. However, for DPPC lipid vesicles, we observed a significant variation in the D_t value for the dyes. The average D_t values for DCM, C480, and C343 are 5, 20, and 40 $\mu m^2/s$, respectively (Figure 9). The variation in D_t value (8-fold from 5 $\mu m^2/s$ for DCM to 40 $\mu m^2/s$ for C343 in DPPC) within lipid bilayers is substantially different from that in bulk water. This probe dependence conclusively supports our contention that the FCS trace arises from dye diffusion within the vesicles. The probe dependence of D_t for the three dyes is attributed to their location. DCM being a highly hydrophobic dye is preferentially located in the buried/nonpolar region within the vesicle and, hence, displays lower mobility. C343, an anionic hydrophilic dye, remains exposed and shows higher mobility. Similar probe dependence of D_t of different dyes has earlier been ascribed to different locations in a polymer gel.[12]

4. Conclusion

FCS studies at a single vesicle level demonstrate a distribution in the D_t values of a given lipid. This indicates the presence of microheterogeneity. The fluctuation in D_t values may be attributed to size and shape variation of single lipid vesicles. It is also observed that there is a distinct variation in the gel and fluid phases studied. The D_t of DCM in the gel phase (~5 $\mu m^2/s$) and the fluid phase (~40 $\mu m^2/s$) are 60 times and 8 times smaller compared to that in bulk water. Also, D_t in the gel phase is 8 times smaller than that in the fluid phase. This displays marked phase dependence of D_t in a lipid. Finally, in a single lipid vesicle, a significant region dependence of D_t was observed when three dyes of different hydrophobicity were used.

Acknowledgment. Thanks are due to Department of Science and Technology, India (Project no. IR/I1/CF-01/2002 and J. C. Bose Fellowship), and the Council of Scientific and Industrial Research (CSIR) for generous research support. S.G., A.A., and S.S.M. thank CSIR for awarding fellowships.

References and Notes

(1) (a) Magde, D.; Elson, E. L.; Webb, W. W. *Biopolymers* **1974**, *13*, 29. (b) Edman, L.; Mets, Ü.; Rigler, R. *Proc. Natl. Acad. Sci. U.S.A.* **1996**, *93*, 6710. (c) Schwille, P.; Bieschke, J.; Oehlenschläger, F. *Biophys. Chem.* **1997**, *66*, 211. (d) Petrasek, Z.; Schwille, P. *Biophys. J.* **2008**, *94*, 1437. (e) Lakowicz, J. R. *Principles of Fluorescence Spectroscopy*, 3rd ed.; Springer: New York, 2006; Chap. 24.

(2) (a) Wohland, T.; Friedrich, K.; Hovius, R.; Vogel, H. *Biochemistry* **1999**, *38*, 8671. (b) Van Craenenbroeck, E.; Engelborghs, Y. *Biochemistry* **1999**, *38*, 5082.

(3) (a) Larson, D. R.; Ma, Y. M.; Vogt, V. M.; Webb, W. W. *J. Cell Biol.* **2003**, *162*, 1233. (b) Pitschke, M.; Prior, R.; Haupt, M.; Riesner, D. *Nat. Med.* **1999**, *4*, 832.

(4) Schwille, P.; Oehlenschelager, F.; Walter, N. G. *Biochemistry* **1996**, *35*, 10182.

(5) (a) Bjorling, S.; Kinjo, M.; Foldes-Papp, Z.; Hagman, E.; Thyberg, P.; Rigler, R. *Biochemistry* **1998**, *37*, 12971. (b) Rigler, R.; Foldes-Papp, Z.; Meyer-Almes, F. J.; Sammet, C.; Volcker, M.; Schnetz, A. *J. Biotechnol.* **1998**, *63*, 97.

(6) (a) Schubert, F.; Zettl, H.; Hafner, W.; Krauss, G.; Krausch, G. *Biochemistry* **2003**, *42*, 10288. (b) Wohland, T.; Friedrich-Benet, K.; Pick, H.; Preuss, A.; Hovius, R.; Vogel, H. In *Single Molecule Spectroscopy*; Rigler, R., Orrit, M., Basche, T., Eds.; Springer: New York, 2002; pp 195–210.

(7) (a) Schuler, J.; Frank, J.; Trier, U.; Schafer-Korting, M.; Saenger, W. *Biochemistry* **1999**, *38*, 8402. (b) Pick, H.; Preuss, A. K.; Mayer, M.; Wohland, T.; Hovius, R.; Vogel, H. *Biochemistry* **2003**, *42*, 877.

(8) Yue, H.; Wu, M.; Xue, S.; Velayudham, S.; Liu, H.; Waldeck, D. H. *J. Phys. Chem. B* **2008**, *112*, 218.

(9) Zettl, H.; Portnoy, Y.; Gottlieb, M.; Krausch, G. *J. Phys. Chem. B* **2005**, *109*, 13397.

(10) Lioi, B. S.; Wang, X.; Islam, M. R.; Danoff, D.; English, D. S. *Phys. Chem. Chem. Phys.* **2009**, *11*, 9315.

(11) Mueller, W.; Koynov, K.; Fischer, K.; Hartmann, S.; Pierrat, S.; Basche, T.; Maskos, M. *Macromolecules* **2009**, *42*, 357.

(12) Ghosh, S.; Mandal, U.; Adhikari, A.; Bhattacharyya, K. *Chem. Asian J.* **2009**, *4*, 948.

(13) Wanka, G.; Hoffmann, H.; Ulbricht, W. *Macromolecules* **1994**, *27*, 4145.

(14) (a) New, R. R. C., Ed. *Liposomes a practical approach*; Oxford University Press: New York, 1990. (b) Kucerka, N.; Kiselev, M. A.; Balgavy, P. *Eur. Biophys. J.* **2004**, *33*, 328.

(15) Gao, F.; Mei, E.; Lim, M.; Hochstrasser, R. M. *J. Am. Chem. Soc.* **2006**, *128*, 4814.

(16) Korlach, J.; Schwille, P.; Webb, W. W.; Feigenson, G. W. *Proc. Natl. Acad. Sci. U.S.A.* **1999**, *96*, 8461.

(17) Dertinger, T.; von der Hocht, I.; Benda, A.; Hof, M.; Enderlein, J. *Langmuir* **2006**, *22*, 9339.

(18) Przybylo, M.; Sykora, J.; Humpolıckova, J.; Benda, A.; Zan, A.; Hof, M. *Langmuir* **2006**, *22*, 9096.

(19) (a) Johnson, J. M.; Ha, T.; Chu, S.; Boxer, S. G. *Biophys. J.* **2002**, *83*, 3371. (b) Schonherr, H.; Johnson, J. M.; Lenz, P.; Frank, C. W.; Boxer, S. G. *Langmuir* **2004**, *20*, 11600.

(20) (a) Feng, Z. V.; Spurlin, T. A.; Gewirth, A. A. *Biophys. J.* **2005**, *88*, 2154. (b) Enders, O.; Ngezahayo, A.; Wiechmann, M.; Leisten, F.; Kolb, H. A. *Biophys. J.* **2004**, *87*, 2522–2531.

(21) (a) Charrier, A.; Thibaudau, F. *Biophys. J.* **2005**, *89*, 1094. (b) Tokumasu, F.; Jin, A. J.; Feigenson, G. W.; Dvorak, J. A. *Ultramicroscopy* **2003**, *97*, 217.

JP911971P